Materials Research Letters

ISSN: 2166-3831 (Online) Journal homepage: www.tandfonline.com/journals/tmrl20

Ultrasonic assisted micro-shear punching of amorphous alloy

Feng Luo, Fei Sun, Kangsen Li, Feng Gong, Xiong Liang, Xiaoyu Wu & Jiang Ma

To cite this article: Feng Luo, Fei Sun, Kangsen Li, Feng Gong, Xiong Liang, Xiaoyu Wu & Jiang Ma (2018) Ultrasonic assisted micro-shear punching of amorphous alloy, Materials Research Letters, 6:10, 545-551, DOI: 10.1080/21663831.2018.1500399

To link to this article: https://doi.org/10.1080/21663831.2018.1500399

© 2018 The Author(s). Published by Informa UK Limited, trading as Taylor & Francis Group

Published online: 24 Jul 2018.

Submit your article to this journal

Article views: 2771

View related articles

View Crossmark data

Citing articles: 8 View citing articles

Full Terms & Conditions of access and use can be found at
https://www.tandfonline.com/action/journalInformation?journalCode=tmrl20

MATER. RES. LETT.
2018, VOL. 6, NO. 10, 545–551
https://doi.org/10.1080/21663831.2018.1500399

MATERIALS RESEARCH LETTERS
Taylor & Francis
Taylor & Francis Group

ORIGINAL REPORT

OPEN ACCESS
Check for updates

Ultrasonic assisted micro-shear punching of amorphous alloy

Feng Luo, Fei Sun, Kangsen Li, Feng Gong, Xiong Liang, Xiaoyu Wu and Jiang Ma

Guangdong Provincial Key Laboratory of Micro/Nano Optomechatronics Engineering, College of Mechatronics and Control Engineering, Shenzhen University, Shenzhen, People's Republic of China

ABSTRACT

Despite the excellent properties, amorphous alloys find limited applications and to find plastic forming ability has been a longstanding problem. In this work, an effective ultrasonic assisted micro-shear punching (UMSP) method is proposed for amorphous alloys. By applying ultrasonic vibration and molten plastics viscous medium, a series of shapes and products with micro-length scale to macro-length scale can be successfully fabricated in 50 ms. Different from traditional crystalline alloys, the amorphous alloys become soft at certain regions during the ultrasonic hammering owing to the unique disordered structures, thereby resulting in the low-stress forming approach.

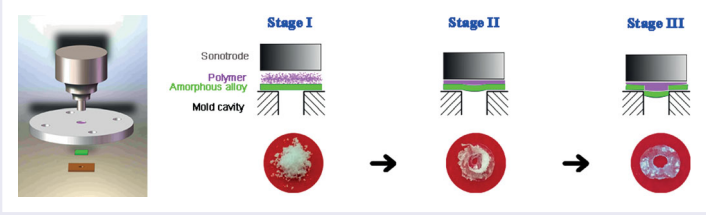

IMPACT STATEMENT

In this work, a new acting mechanism was found between amorphous alloy and the high-frequency vibration, providing an efficient approach for the fabrication of amorphous alloy products.

ARTICLE HISTORY
Received 27 March 2018

KEYWORDS
Micro-shear punching; amorphous alloys; ultrasonic hammering; flexible punch

1. Introduction

Amorphous alloys have aroused wide interests since they were discovered in the 1960s [1]. The high specific strength, large elastic strain limit and excellent wear and corrosion resistances along with other remarkable engineering properties made these materials very promising in many applications [1–14]. However, being the Achilles' heel of amorphous alloys, the lack of macroscopic ductility at low temperature (below the glass transition temperature) has greatly limited their applications as structural materials. As long as the stress exceeds the yield strength of the amorphous alloys, local shear will occur, and the unlimited propagation of the shear bands will lead to the catastrophic damage [15]. Owing to the intrinsically brittle peculiarity, amorphous alloys reveal the 'unfriendly' side to the conventional cold plastic forming techniques, such as extrusion, drawing and punching. Therefore, to develop the plastic forming techniques have been a longstanding major issue for the practical use of these materials.

Shear punching is a metal forming process that forces a tool through the workpiece to create products via shearing, e.g. blanking or piercing. As one of the cheapest methods for medium to high production volumes, shear punching is widely applied in the industry [16]. Materials that can be punched including aluminium, brass, copper and their alloys, stainless steels and even plastics [16], have good ductility and low strength. Many efforts have been tried to fabricate amorphous alloy products by the plastic deformation method [17], in which shear punching is demonstrated to be an efficient one [18–22]. However, the shear punching of amorphous alloys just focused on the macroscopic shapes or products, micro-punching of the same alloys, which is in great demand in the micro-device fields, still remains uninvestigated. Furthermore, rigid punch was used in previous work on

CONTACT Jiang Ma majiang@szu.edu.cn Guangdong Provincial Key Laboratory of Micro/Nano Optomechatronics Engineering, College of Mechatronics and Control Engineering, Shenzhen University, Shenzhen 518060, People's Republic of China

© 2018 The Author(s). Published by Informa UK Limited, trading as Taylor & Francis Group.
This is an Open Access article distributed under the terms of the Creative Commons Attribution License (http://creativecommons.org/licenses/by/4.0/), which permits unrestricted use, distribution, and reproduction in any medium, provided the original work is properly cited.

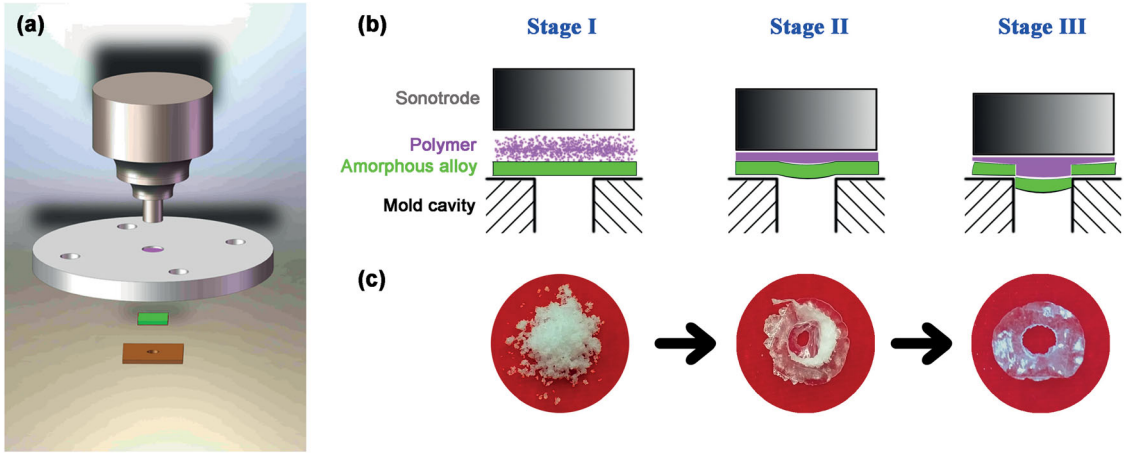

Figure 1. (a) Illustration of the UMSP method for amorphous alloys. (b) Different stages during the UMSP. (c) The photographs of the plastic powder at different stages.

the punching of amorphous alloys, as a result, a large force was required to avoid the energy waste and poor dimensional accuracy [18,22].

In this paper, an effective ultrasonic assisted micro-shear punching (UMSP) method is proposed for amorphous alloys. This method comprehensively applies ultrasonic vibration and molten plastic viscous medium in the punching process of amorphous alloys. By using the UMSP, a series of micro-circular holes with diameters ranging from 300 μm to 750 μm were obtained in 50 ms. In addition, more products with complex shapes also have preliminary experimental results, showing that the UMSP is an efficient and cost-saving approach to produce amorphous alloy parts.

2. Experimental

2.1. Materials and mould preparation

The $Fe_{78}Si_9B_{13}$ (at.%) amorphous alloy ribbons with a thickness of 25 μm were chosen for this work. The composition has an average tensile strength of 1640 ± 35 MPa [23]. It is difficult to deform this material into products by conventional plastic deformation method because of its high strength and lack of plasticity. For the convenience of UMSP, the amorphous alloy ribbon was cut into a square with a side length of 10 mm. The micro-moulds of different shapes for the present research are prepared by a low-speed wire electrical discharge machining (WEDM; SODICK AP250L). The diameter of the wire is 50 μm.

2.2. Characterizations

The amorphous nature of the Fe-based amorphous alloys was ascertained by x-ray diffraction (XRD; Rigaku Mini-Flex600) with Cu Kα radiation and differential scanning calorimetry (DSC; Perkin–Elmer DSC-8000) at a heating rate of 20 K/min. The micro-morphologies of the moulds and the punched products were collected on a scanning electron microscope (SEM; FEI QUANTA FEG 450) instrument.

2.3. Experimental set-up

The basic principle of the UMSP method for amorphous alloy ribbons is schematically drawn in Figure 1(a). Each component is marked in detail. To make it clear, Figure 1(b) presents the process in 'slow motion'. A thin Fe-based amorphous alloy sheet with an area of 10 mm × 10 mm is placed on the mould. Then, the plastic powder (Ethylene Vinyl Acetate; EVA) with an average diameter of 300 μm is put into the stock bin of the pressure plate (Stage I). The volume of the used plastic powder is about 50 mm^3, half of the stock bin. When the punch drops, the ultrasonic vibration starts and acts on the plastic powder, making it melt rapidly into the fluid state. In the present research, the frequency of the vibration is 20,000 Hz and the amplitude is 40 μm, resulting in a velocity of 3.2^*10^7 μm/s during the ultrasonic vibration. The molten plastic acts as the flexible punch and pressure transmission medium, it transmits the main force and the ultrasonic vibration to the thin sheet amorphous ribbons (Stage II). During the constant ultrasonic hammering, the workpiece is squeezed into the mould cavity by the uniform plastic medium under the pressure of the punch, and a certain shape was punched out from the metallic sheet (Stage III). Figure 1(c) presents the photographs of the plastic powder at different stages.

3. Result and discussions

3.1. Surface morphology after UMSP

To investigate the governing mechanism of the UMSP, micro-moulds with holes of diameters ranging from

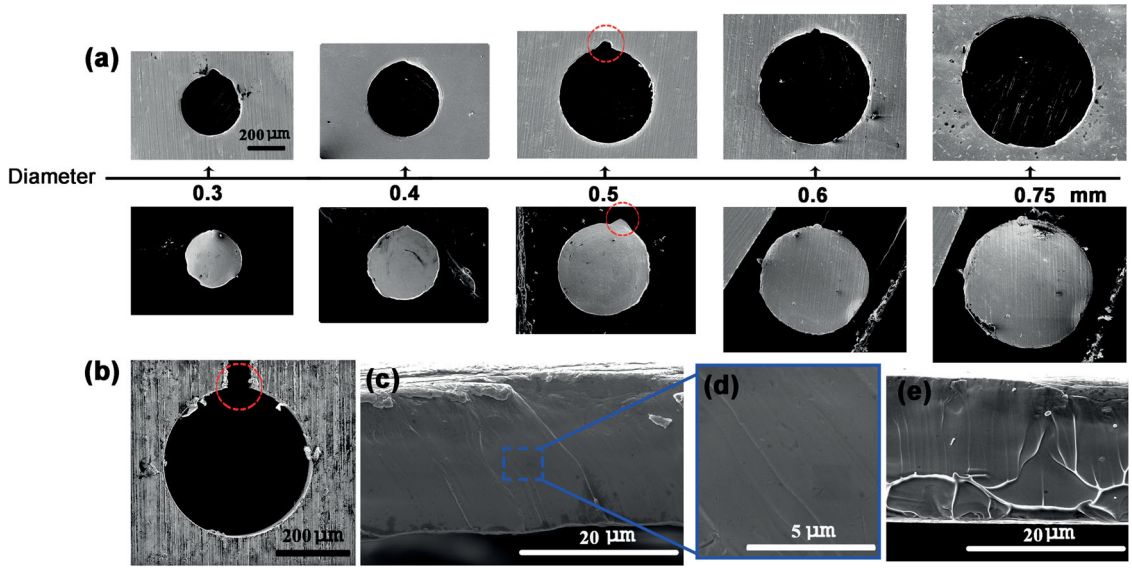

Figure 2. (a) Top row: SEM images of the ribbons with micro-holes after UMSP; Bottom row: the punch-out amorphous alloy discs. All the images share the same scale bar. (b) The mould cavity prepared by a low-speed WEDM. (c) The cross-section of amorphous alloys after UMSP. (d) The magnification of (c). (e) The cross-section of the tensile amorphous alloy sample.

0.3 mm to 0.75 mm were fabricated and the UMSP of Fe-based amorphous alloy ribbons was conducted. The top row in Figure 2(a) presents SEM images of the ribbons with micro-holes after the UMSP, and the bottom row shows the punch-out discs. It can be seen that they are in good accordance with each other. The coincidence rate in dimensions is close to 100% by comparing the areas of the micro-holes and the discs. The results indicate that the UMSP method is capable of producing amorphous alloys rapidly with fine dimensional quality.

There is one thing that should be noted that a tiny corner breakage can be found on the micro-holes and the corresponding punch-out discs (See the highlighted region in Figure 2(a)). It is not the defect caused by the UMSP but caused by the mould cavity. As it is mentioned above, the micro-moulds were prepared by a low-speed WEDM, an inevitable thin gap is left on the mould to release the wire, which can be found in the highlight region of Figure 2(b). It is the gap that caused the corner breakage.

The morphology of the cross-section after UMSP was observed and presented in Figure 2(c). Figure 2(d) shows the magnification of Figure 2(c). For comparison, the cross-section of the tensile sample is presented in Figure 2(e). Clearly, the fracture surfaces of UMSP and tension are quite different, the former is neat and smooth, the latter displays the typical river-like patterns. Normally, the cross-section can be divided into several feature zones for traditional shear punch, including rollover zone, shear zone, fracture zone and burr zone. However, no such features are found in Figure 2(c, d). The neat and smooth cross-section may indicate a different mechanism during the UMSP of amorphous alloys, which will be discussed below.

3.2. UMSP mechanism for amorphous alloys

As for the crystalline alloys, the traditional punching mechanism can be expressed by the following equation: [24]

$$P = \frac{4T\sigma}{d}, \tag{1}$$

where P, T, σ and d are the required punching pressure, workpiece thickness, tensile strength of the workpiece material and hole diameter, respectively. According to the above equation, the required punching force P is 547, 410, 328, 273 and 219 MPa for the holes of diameters 0.3, 0.4, 0.5, 0.6 and 0.75 mm, respectively. However, in the present research, the acting punching pressure for these holes is 95, 86, 64, 57 and 40 MPa, respectively. The punching pressure with a success rate of 100% versus diameter is plotted in Figure 3(a). It should be noted that the above stress reaches just preset average values, stress fluctuations could happen during the UMSP process owing to the vibration of the sonotrode.

Using the nonlinear fitting, the data points in Figure 3(a) can be fitted by the following power equation:

$$P = 31d^{-1}. \tag{2}$$

It can be seen the actual punching pressure was much lower than the calculated values. That is to say, Equation

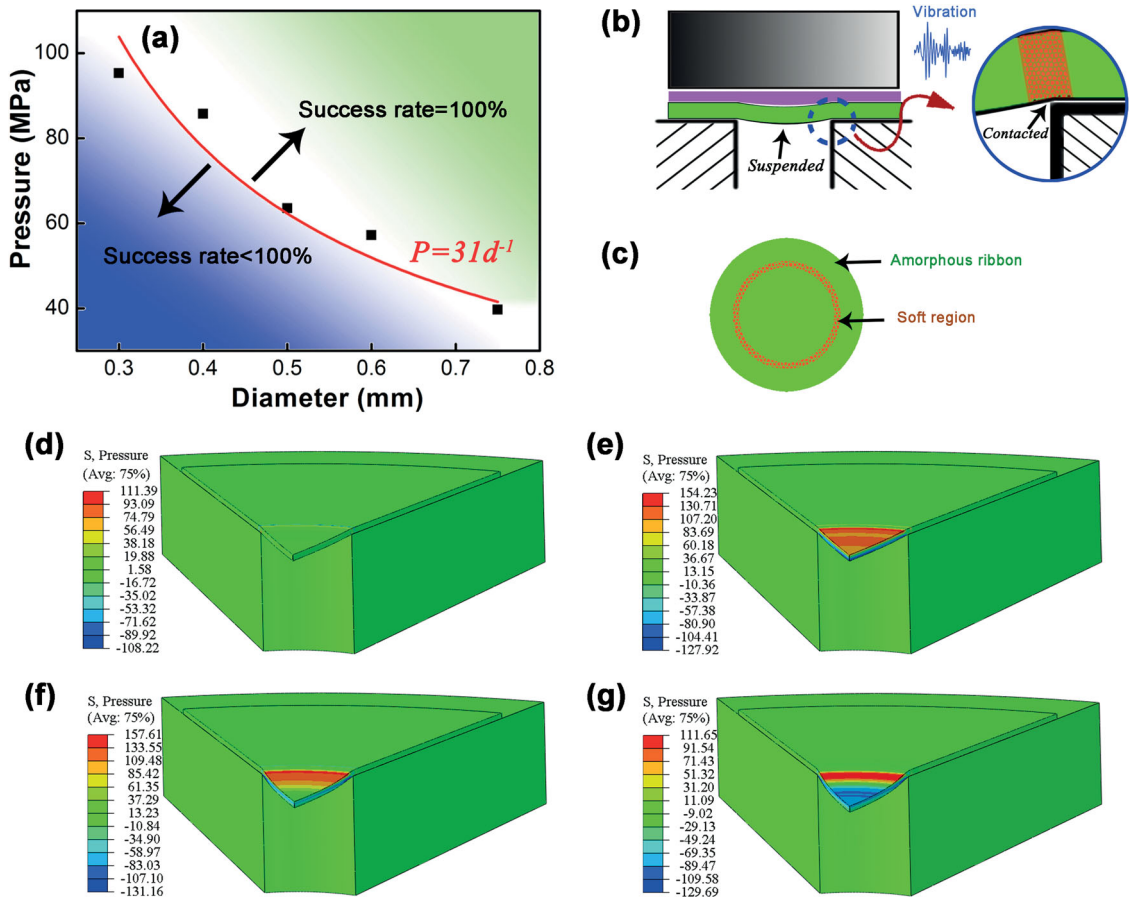

Figure 3. (a) The punching pressure with a success rate of 100% versus hole diameter. The fitted line shows the tendency. (b) The details of the amorphous alloy around the mould edge during the UMSP. (c) The soft region of the amorphous ribbon from top view during the ultrasonic hammering. (d–g) show the typical stages of deformations with contours of pressure distribution (MPa).

(1) is not suitable for the description of UMSP. This is reasonable for amorphous alloys under high-frequency ultrasonic vibration. As a class of disordered materials, amorphous alloys were considered as the combination of elastic matrix and the dispersed liquid-like sites. Owing to such unique structures, the specific liquid-like regions could couple with the high-frequency hammering and absorb the hammering energy, resulting in the activation of α-relaxation with the hammering progressed. It had been proved that the thermoplastic forming of amorphous alloys could be achieved by the ultrasonic hammering [25].

As illustrated in Figure 3(b), during the UMSP, the central part of the amorphous ribbons was suspended, so the ultrasonic hammering energy was dissipated by the elastic vibration of this part. However, when it comes to the mould edge, the elastic vibration was confined, hence the energy was stored and activated the viscous flow of amorphous alloy ribbons at the mould edge part. The magnified illustration in 3(b) reveals the micro-process. Figure 3(c) schematically draws the soft region of the amorphous ribbon from top view. That is to say, the amorphous ribbon gets soft along with the mould edge because of the ultrasonic hammering, leading to the low stress punching of this material. Let us get back to the cross-section morphology in Figure 2(c, d), the smooth section could be the evidence of the viscous flow. The deformation behaviour of UMSP is different from that shown in the simple mechanical tests. During UMSP, the amorphous ribbon will first get soft at certain regions along the mould edge under a low stress but high-frequency vibrations, and a specific shape was punched out, forming a smooth fracture surface. However, during the simple mechanical tests, the amorphous alloy ribbon will store the elastic energy until the stress reaches a very high value, and the shear bands initiate, leading to the fracture of the sample. At the same time, vein pattern forms owing to the prolongation of shear bands in the fracture process. Therefore, the UMSP and the simple mechanical tests could be considered as the integral and local softening inside of the amorphous ribbons, respectively. Assuming that the amorphous alloy was passed into a viscous state with a viscosity of η, the driven stress σ required for the liquid to undergo a strain ϵ in a period

of time t can be expressed as follows:

$$\sigma = 3\eta\frac{\varepsilon}{t}. \tag{3}$$

For the shear punching process, the deformation of the viscous region should equal the thickness of the amorphous ribbon T to ensure the falling off of the shear punching product; therefore, the equivalent strain ϵ equals 1. By substituting Equation (3) into Equation (1), we can obtain the following:

$$P = \frac{12T\eta}{td}. \tag{4}$$

In this work, $T = 25\,\mu$m, $t = 0.05$ s. Combining Equationss (1 and 4) together, it can be calculated that $\eta = 5.2\times10^3\cdot$Pa s, just in the supercooled liquid region of amorphous alloys [26]. These results indicate that the UMSP of amorphous alloys follows a different mechanism with the traditional punching technique and crystalline materials such as copper and stainless steel.

3.3. Simulation

To investigate the stress distribution on the amorphous alloy ribbon during the UMSP, the finite element method (FEM) was carried out with the perfectly plastic model due to no work-hardening for most amorphous alloys. The simulation was conducted using the ABAQUS/Explicit, the parameters used were as follows: diameter of the micro-hole was 0.75 mm, the amplitude of the ultrasonic punch and the pressure were 40 μm and 40 MPa, respectively. The amorphous alloy ribbon and polymer powder were treated as Lagrange deformable bodies which were meshed with 12,900 and 10,800 elements, respectively. During the simulation, the polymer is considered as a low modulus (modulus = 0.25 GPa) stress transmitter, the elastic modulus, density, expansion coefficient and Poisson's ratio of the amorphous ribbon were 130 GPa, 7.18 g/cm^3, 1.3×10^{-5} K^{-1} and 0.31, respectively, according to the experimental results.

Figure 3(d–g) shows the typical stages of deformations with contours of the pressure distribution. It can be seen that the high stress gradient zone is located on the sharp corner of mould. The localized stress distribution strengthens the softening effect of amorphous alloy ribbon during UMSP. After the workpiece gets soft around the corner of the mould, a target plate will be sheared off easily, thus the punching is realized.

3.4. Micro–macro-scale UMSP of amorphous alloys

The proposed UMSP is a fast and low-cost method to find a solution for the widespread engineering application of amorphous alloy products. To validate the availability of this method, several different shapes with micro-length scale to macro-length scale were designed and corresponding products were fabricated. Figure 4(a) presents the photos of amorphous alloy ribbons after

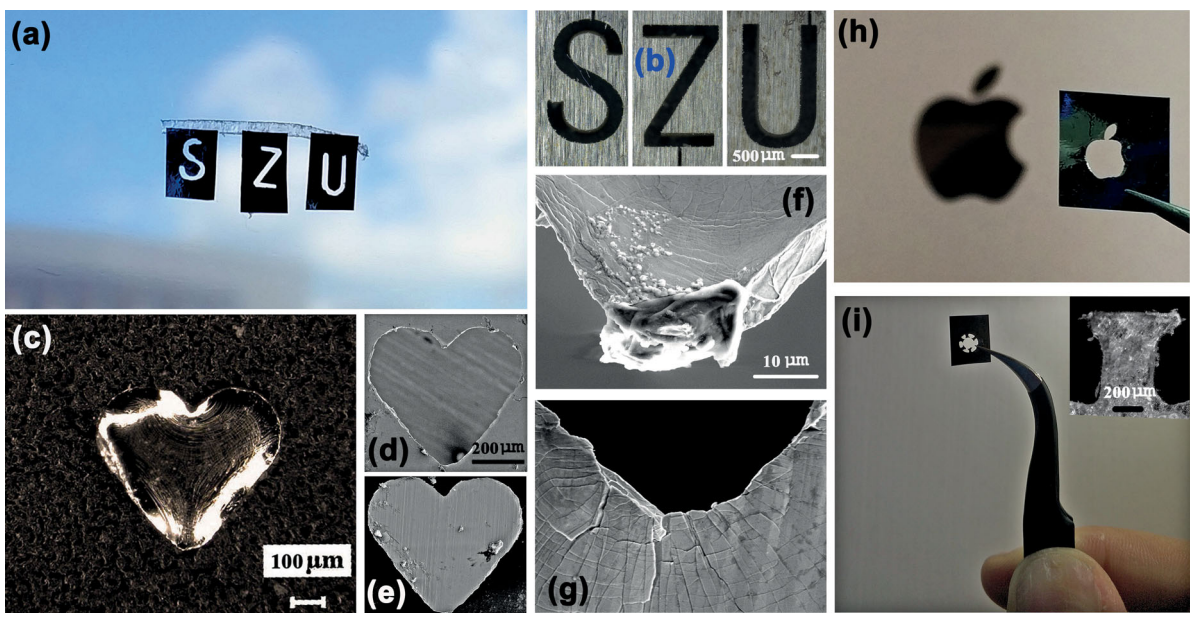

Figure 4. (a) The photos of amorphous alloy ribbons after punching out the capital letters 'S', 'Z' and 'U', which stands for the initial letters of 'ShenZhen University'. (b) The stereomicroscope images of the letter moulds. (c) The optical microscope image of the heart-shaped product. (d and e) The SEM images of the ribbon with a heart hole and the heart-shaped product. (f and g) The magnified images of (d and e). (h) A macro-scale UMSP Apple's logo compared with the real logo on iPhone 6. (i) A typical stator core fabricated by the UMSP method in 0.05 s. (d–g) share the same scale bar.

punching out the capital letters 'S', 'Z' and 'U', which stands for the initial letters of 'ShenZhen University'. The stereomicroscopic images of the moulds are shown in Figure 4(b), the line width of the letters is about 350 μm.

A more complex heart-shaped product was also tried, and Figure 4(c) gives the optical microscopic image, no obvious defects can be found. To examine the details, the SEM images of the ribbon with a heart hole and the heart-shaped product are presented in Figure 4(d, e), respectively. Clearly, they are in good dimensional accordance with each other. Taking a more careful look of Figure 4(d, e), we can see the complete tip in Figure 4(f) and the corresponding nook in Figure 4(g). The minimum corner radius is 10 μm here, and this is the most difficult part to punch. Furthermore, multiple shear bands can be found in this area, indicating the complex stress state of the amorphous alloy ribbon during UMSP.

Except the micro-scale features, a macro-scale Apple's logo was also successfully fabricated. Figure 4(h) shows the photo of the logo compared with the real logo on iPhone 6. The length and width of the logo are several millimetres with sharp nooks on it, we can find the neat profile of the logo. As we know, the Fe-based amorphous ribbons show excellent soft magnetic properties and are finding wider applications in the electronic transformer devices. However, how to fabricate such products efficiently from ribbons has been a restricting problem. A compromising method is to use the wire electron discharge machining (WEDM) to cut them into specific shapes, which is time-consuming and expensive. Figure 4(i) presents a typical stator core fabricated by the UMSP method. The inset in Figure 4(i) reveals the details of the stator core. It should be noted that the time cycle of this product is 0.05 s, far shorter than that of the WEDM method. These results indicate that the UMSP method for amorphous alloys could have extensive potential applications.

4. Conclusions

In summary, this work proposed a UMSP method for the plastic forming of amorphous alloys. By using such a method, a series of shapes and products with a micro-length scale to macro-length scale can be successfully fabricated in 50 ms. The forming mechanism is different from that of traditional crystalline alloys. Owing to the ultrasonic hammering, the amorphous alloy gets soft at certain regions, resulting in the low-stress forming approach. Our results provide a fast and low-cost energy-saving method for the massive production of amorphous alloy devices and throw light on the widespread engineering applications of these materials.

Disclosure statement

No potential conflict of interest was reported by the author(s).

Funding

The work was supported by the National Natural Science Foundation of China [Grant Nr. 51501116, 51775351, 51205258, 51405306], Natural Science Foundation of Guangdong Province [Grant Nr. 2016A030310043, 2017A030313311], the Shenzhen Science and Technology Innovation Commission [Grants No. JCYJ20170412111216258, JCYJ20160520164903055, JCYJ20150324140036865].

References

[1] Klement W, Willens RH, Duwez P. Non-crystalline structure in solidified gold–silicon alloys. Nature. 1960;187:869–870.
[2] Johnson WL. Bulk glass-forming metallic alloys: science and technology. MRS Bulletin. 1999;24(10):42–56.
[3] Wang WH, Dong C, Shek CH. Bulk metallic glasses. Mater Sci Eng: R: Reports. 2004;44(2):45–89.
[4] Inoue A. Stabilization of metallic supercooled liquid and bulk amorphous alloys. Acta Mater. 2000;48(1):279–306.
[5] Chen HS. Glassy metals. Rep Prog Phys. 1980;43(4):1–5.
[6] Lu ZP, Liu CT. A new glass-forming ability criterion for bulk metallic glasses. Acta Mater. 2002;50(13):3501–3512.
[7] Peker A, Johnson WL. A highly processable metallic glass: $Zr_{41.2}Ti_{13.8}Cu_{12.5}Ni_{10.0}Be_{22.5}$. Appl Phys Lett. 1993;63(17):2342–2344.
[8] Demetriou MD, Launey ME, Garrett G, et al. A damage-tolerant glass. Nat Mater. 2011;10(2):123–128.
[9] Schuh CA, Hufnagel TC, Ramamurty U. Mechanical behavior of amorphous alloys. Acta Mater. 2007;55(12):4067–4109.
[10] Telford M. The case for bulk metallic glass. Mater Today. 2004;7(3):36–43.
[11] Guan PF, Chen MW, Egami T. Stress-temperature scaling for steady-state flow in metallic glasses. Phys Rev Lett. 2010;104(20):205701-1–205701-4.
[12] Nieh T, Wadsworth J, Liu C, et al. Plasticity and structural instability in a bulk metallic glass deformed in the supercooled liquid region. Acta Mater. 2001;49(15):2887–2896.
[13] Schroers J. Processing of bulk metallic glass. Adv Mater. 2010;22(14):1566–1597.
[14] Greer AL. Metallic glasses. Science. 1995;267(5206):1947–1953.
[15] Liu YH, Wang G, Wang RJ, et al. Super plastic bulk metallic glasses at room temperature. Science. 2007;315(5817):1385–1388.
[16] Kalpakjian S, Schmid SR. Manufacturing engineering and technology. Singapore: Pearson Publications; 2014. p. 1–100.
[17] Suryanarayana C, Inoue A. Bulk metallic glasses. London: CRC Press; 2011. p. 20–100.
[18] Huang Y, Wang D, Fan H, et al. Shear punching of a Ti-based bulk metallic glass. Materials Science and Engineering: A. 2013;561:220–225.
[19] Liu L, Dai L, Bai Y, et al. Characterization of rate-dependent shear behavior of Zr-based bulk metallic glass using shear-punch testing. J Mater Res. 2006;21(1):153–160.

[20] Jeong HG, Kim WJ, Bae JC, et al., editors. Hole punching onto the $Zr_{65}Al_{10}Ni_{10}Cu_{15}$ BMG sheet fabricated by squeeze casting. Mater Sci Forum;2005: Trans Tech Publ.
[21] Guduru R, Darling K, Kishore R, et al. Evaluation of mechanical properties using shear–punch testing. Mater Sci Eng: A. 2005;395(1):307–314.
[22] Takahashi F, Nishimura T, Suzuki I, et al. A method of blanking from amorphous alloy foils using rubber tool. CIRP Annals. 1991;40(1):315–318.
[23] El-Shabasy AB, Hassan HA, Lewandowski JJ. Effects of composition changes on strength, bend ductility, toughness, and flex-bending fatigue of iron-based metallic glass ribbons. Metall Mater Trans A. 2012;43(8):2697–2705.
[24] Geiger M, Vollertsen F, Kals R. Fundamentals on the manufacturing of sheet metal microparts. CIRP Ann. 1996;45(1):277–282.
[25] Ma J, Liang X, Wu X, et al. Sub-second thermoplastic forming of bulk metallic glasses by ultrasonic beating. Sci Rep. 2016;5:17844-1–17844-6.
[26] Busch R, Schroers J, Wang WH. Thermodynamics and kinetics of bulk metallic glass. MRS Bulletin. 2007;32(08):620–623.